Integrated network pharmacology and cellular assay reveal the biological mechanisms of Limonium sinense (Girard) Kuntze against breast cancer

Hualong Zhao
Yancheng Teachers' University
Siyuan Wang
University of Southampton
Philip T.F. Williamson
University of Southampton
Rob M. Ewing
University of Southampton
Xinhui Tang
Yancheng Teachers' University
Jialian Wang
Yancheng Teachers' University
Yihua Wang (yihua.wang@soton.ac.uk)
University of Southampton

Research Article

Keywords: Limonium Sinense (Girard) Kuntze, Network pharmacology, breast cancer, Gene Expression Omnibus, Apigenin

Posted Date: June 20th, 2023

DOI: https://doi.org/10.21203/rs.3.rs-3068701/v1

Abstract

Background

Limonium Sinense (Girard) Kuntze (*L. sinense*) has been widely used for the treatment of anaemia, bleeding, cancer, and other disorders in Chinese folk medicine. Although *L. sinense* has shown promising inhibitory effects on breast cancer, the exact mechanism underlying its anticancer properties remains unclear.

Methods

The active ingredients of *L. sinense* were collected from published literature, and the potential targets related to *L. sinense* were obtained from public databases. Gene Ontology (GO), Kyoto Encyclopedia of Genes and Genomes (KEGG) and DisGeNET enrichment analyses were performed to explore the underlying mechanisms. Molecular docking, cellular experiments, and Gene Expression Omnibus (GEO) datasets were employed to further evaluate the findings.

Results

A total of 15 active ingredients of *L. sinense* and their corresponding 389 targets were obtained. Enrichment and network analyses revealed that the biological effects of *L. sinense* were primarily associated with breast cancer. Apigenin within *L. sinense* was found to potentially play a key role against cancer. Cellular experiments demonstrated that the *L. sinense* ethanol extract (LSE) exhibited a significant growth inhibitory effect on multiple breast cancer cell lines in both 2D and 3D cultures. Additionally, analysis of GEO datasets validated the significant enrichment of breast cancer and several cancer-related pathways upon treatment with Apigenin in human breast cancer cells.

Conclusion

This study predicts the biological activities of *L. sinense* and demonstrates the inhibitory effect of LSE on breast cancer cells, highlighting the potential application of *L. sinense* in cancer treatment.

Introduction

Limonium sinense (Girard) Kuntze (*L. sinense*), also known as *Latouchea Fokiensis* and *Limoniumspp*, is an endemic plant species with commercially important value in Chinese medicine [1]. *L. sinense* mainly grows in the seashores and salt marshes regions of mainland China, western Taiwan of China and Ryukyus islands in Japan [2, 3]. In Chinese folk medicine, *L. sinense* is commonly used for the treatment of bleeding, fever, hepatitis, haemostasis, anaemia, menorrhagia, irregular menstruation and other disorders [4, 5]. Studies have reported that the polysaccharides derived from the root of *L. sinense* exhibit potent anti-tumour and immunomodulatory activities with low toxicity, effectively inhibiting the growth of tumours in mice [6]. Notably, LSP21, a polysaccharide separated from crude *L. sinense* polysaccharides, has demonstrated remarkable anti-tumour effects by inhibiting cell proliferation and inducing cell death

[7]. Furthermore, *L. sinense* extracts have shown hepatoprotective activity against carbon tetrachloride and D-galactosamine intoxication in rats, with the underlying mechanism being associated with mitochondrial protection [2, 8, 9]. Other studies revealed significant anti-viral activity of *L. sinense*, and compounds such as gallic acid, samarangenin B and myricetin derived from *L. sinense* exhibited significant inhibitory effects against viral infections [10–12]. Our previous study [13] have found a significant inhibitory effect of the water extract of *L. sinense* on multiple types of human breast cancer cells. However, further underlying mechanisms of the pharmacological activities of *L. sinense* still remain to be elucidated.

More than 40 chemical compounds have been identified from *L. sinense*, most of which are flavonoids [12, 14]. However, there are few studies investigating the biological activities of these active ingredients and their associated mechanisms in *L. sinense.* In this study, network pharmacology and *in vitro* cellular experiments were employed to gain insights into the molecular basis of the therapeutic effects of *L. sinense*. We first explored the active ingredients and possible targets of *L. sinense*. By constructing the Compound-Target-Pathway network, a hub connection was identified from the network. Molecular docking, cellular experiments and Gene Expression Omnibus (GEO) datasets were further performed to validate the findings from network pharmacology results. The detailed technical strategy of this study is shown in Fig. 1.

Materials and methods

Screening of active compounds and the targets L. sinense

L. sinense is not included in the Traditional Chinese Medicine Systems Pharmacology Database and Analysis Platform (TCMSP) or the Encyclopedia of Traditional Chinese Medicine (ETCM) platform, which are two systems pharmacology platforms that allow users to explore the relationships or build networks among drugs, targets and diseases [15, 16]. The compounds of *L. sinense* were therefore obtained from the published literature. Active compounds were screened using the SwissADME database (http://swissadme.ch), based on the *Lipinski*'s rule of five [17] and *Veber*'s rule [18]. Then, the corresponding targets of the active compounds of *L. sinense* were obtained from SwissTargetPrediction.

Construction of Protein-Protein interaction (PPI) network

The STRING (https://cn.string-db.org) database was utilized to analyse protein-protein interaction data. The species were limited to “Homo sapiens”, and an interaction score threshold of 0.4 was applied. Then, the obtained Protein-Protein interaction (PPI) network from the STRING database was visualized by using Cytoscape v3.9.1 software. The core nodes were selected based on the median values of three parameters in the interaction network: “Degree” which indicates the number of links to one node and reflects how often one node interacts with other nodes [19], “Betweenness Centrality” which quantifies the extent to which a node lies on paths between other nodes [20], and “Closeness Centrality” which measures the average distance from a node to other nodes [21]. The level of the three parameters

represents the topological importance of the nodes in the interaction network, with more important nodes outputting higher values in the network [22].

Enrichment analysis

Gene ontology (GO) term and Kyoto Encyclopedia of Genes and Genomes (KEGG) pathway enrichment analysis of the compound targets were generated through GSEApy package, a comprehensive package for performing gene set enrichment analysis within the Python environment [23]. The GSEApy source code is freely available at https://github.com/zqfang/GSEApy. Detailed information regarding the specific GSEApy codes employed in this study can be found in the Supplementary methods section of the article. Diseases associated with the hub targets were enriched by using the disgenet2r package (*version 0.99.3*) in R [24], the specific R codes for performing the enrichment analysis of disgenet2r package are available in the Supplementary methods section of the article.

Network construction

In this process, network construction was performed as follows: First, the Compound-Target network (CT network) was built based on the active compounds *L. sinense* of and their potential targets. Next, the Pathway-Target network (PT network) was constructed by selecting the top 20 enriched KEGG pathways and their associated targets. Finally, a Compound-Target-Pathway network (CTP network) was established by integrating the CT network, PT network and the core targets identified from the PPI network. All visualized network graphs were created using Cytoscape v3.9.1 software. The hub network was screened by using Cytohubba [25], a degree algorithm based Cytoscape plug-in.

Molecular docking

The crystal structure of AKT1 (PDB ID: 3O96), EGFR (PDB ID: 1XKK), SRC (PDB ID: 3EL8), ESR1 (PDB ID: 5ACC), GSK3B (PDB ID: 3I4B) and PTGS2 (PDB ID: 6COX) were downloaded from Protein Data Bank (https://www.rcsb.org/). Compound structure of Apigenin was downloaded from PubChem (https://pubchem.ncbi.nlm.nih.gov/). The docking studies were performed by PyRx Autodock VINA tool (v0.8). A grid box was set to cover the active site of crystal structure with an exhaustiveness of 8. The best compound with highest binding affinity (kcal/mol) was selected and visualized by using Discovery Studio (version 2021 Client) and PyMOL.

Preparation of L. sinense ethanol extract (LSE)

Healthy whole plants of *L. sinense* were collected from the coastal region in Jiangsu, eastern China (33°09'33.0" N, 120°46'40.4" E). The whole plants were washed, and subsequently oven-dried at 60°C until the weight was constant. After drying, the plants were crushed and extracted with 95% ethanol at 95°C for 2 hours at 1:400 (m/v) ratio. The extract process was repeated 3 times under the same conditions. The extracts were then put to suction filtration, rotary evaporated, and freeze-dried to powder. The powder was aliquoted and stored at − 20°C until future use when extracts were diluted with dimethylsulfoxide (DMSO) and filtered through a 0.45 μm filter (Millipore filter membranes, Merck, UK).

Cell culture and reagents

Sources of cell lines and culture conditions were reported earlier [26–28]. HCC1806, HCC1395 and HCC1937 cells were maintained in Roswell Park Memorial Institute (RPMI) 1640 medium, (Gibco® by Life Technology) with 10% fetal bovine serum (FBS) and 1% (v/v) penicillin/streptomycin, (Gibco® by Life Technology). MCF10A, BT20, MDA-MB-157, MDA-MB-231 and MDA-MB-468 cell lines were maintained in Dulbecco's modified Eagle's medium (DMEM) (Gibco® by Life Technology) with 10% FBS and 1% (v/v) penicillin/streptomycin. All cells were kept at 37°C and 5% CO_2. No mycoplasma contamination was detected in the cell lines used. In 3D culture, cells were seeded in 96-well ultralow attachment plate in 100 µl at plating densities between 3,000 and 7,000 cells/well. Cells were cultured in 1:1 DMEM:F12, (Gibco® by Life Technology) media plus 1% P/S, 2% B27 (Gibco® by Life Technology), 20 ng/ml epidermal growth factor (EGF), (PEPROTECH) and 20 ng/ml basic fibroblast growth factor (bFGF) (PEPROTECH) at 37°C and 5% CO_2 for 14 days. After the incubation period, the images were taken using with × 40 magnification.

Cell viability assay

Cell viability assays was performed as previously described [26]. Cells were plated into 96-well plate with a density of 8000 cells/well. CellTiter-Glo® Luminescent cell viability assay (Promega) was performed 24h or 48h after treatment according to the manufacturer's protocol using GloMax® Discover Microplate Reader (Promega). For cell viability in 3D cultures, 100 µl of CellTiter-Glo® reagent was added into each well and incubated at room temperature for 1h, followed by measurement.

GEO datasets analysis

GEO datasets on human breast cancer cells treated with Apigenin were screened, with publication dates prior to 01/05/2023 in the National Centre for Biotechnology Information (NCBI) GEO platform. The obtained datasets were further screened with the following criteria: 1) mRNA expression data; 2) Homo sapiens samples; 3) Breast cancer cells; 4) minimum 3 biological replicates. Duplicate datasets were removed. Datasets with fewer than 10,000 genes were excluded to balance the number of analysed genes and sample size. Microarray probe IDs were translated to gene symbols according to the GPL annotation files provided in the GEO database. Probes mapped to multiple gene symbols were removed and genes mapped to multiple probe IDs were summarized by calculating the mean. Expression data of the same conditions from multiple datasets were integrated (R codes for obtaining the raw data of GEO datasets are shown in Supplementary materials). Genes with P value less than 0.05 and $|Log_2FoldChange|$ above 1 were considered as differentially expressed genes (DEGs). DEGs of each GEO datasets were obtained by GEO2R in the GEO platform.

Statistical analysis

Statistical analyses were performed in GraphPad Prism v7.02 (GraphPad Software Inc, San Diego, CA) unless otherwise indicated. No data were excluded from the studies and for all experiments, all attempts at replication were successful. For each experiment, sample size reflects the number of independent

biological replicates and is provided in the figure legend. Statistical analyses of single comparisons of two groups utilized Student's t-test or Mann-Whitney U-test for parametric and non-parametric data respectively. Where appropriate, individual t-test results were corrected for multiple comparisons using the Holm-Sidak method. For multiple comparisons, one-way or two-way analysis of variance (ANOVA) with Dunnett's multiple comparison test or Kruskal-Wallis analysis with Dunn's multiple comparison test were used for parametric and non-parametric data, respectively. Results were considered significant if $P < 0.05$, where *$P < 0.05$, **$P < 0.01$, ***$P < 0.001$.

Results

Identification of active compounds and targets of L. sinense

Based on the available published literature, a total of 42 natural compounds have been identified from *L. sinense* (Supplementary Table 1). Out of these compounds, 15 have met the *Lipinski*'s rule of five and *Veber*'s rule and defined as the active compounds of *L. sinense* (Table 1). 389 targets associated with these 15 active compounds were obtained after removing duplicate values (Supplementary Table 2). The CT network revealed that all 15 bioactive compounds exhibited relatively high values of Degree, Betweenness Centrality (BC) and Closeness Centrality (CC) within the network (Fig. 2; Supplementary Table 3), showing significant connectivity and potential importance of these compounds in the overall network.

Table 1
Detailed information on active compounds inL. sinense

Compound Name	Molecular weight	nRB	nHA	nHD	TPSA	LogP
Gallic acid	170.12	1	5	4	97.99	-0.16
Ethyl gallate	198.17	3	5	3	86.99	0.49
Apigenin	270.24	1	5	3	90	0.52
Naringenin	272.25	1	5	3	86.99	0.71
Luteolin	286.24	1	6	4	111.13	-0.03
Kaempferol	286.24	1	6	4	111.13	-0.03
Eriodictyol	288.25	1	6	4	107.22	0.16
(+)-Catechin	290.27	1	6	5	110.38	0.24
N-trans-caffeoyltyramine	299.32	6	4	4	89.79	1.65
Quercetin	302.24	1	7	5	131.36	-0.56
Morin	302.24	1	7	5	131.36	-0.56
Homoeriodictyol	302.28	2	6	3	96.22	0.41
N-trans-feruloyltyramine	313.35	7	4	3	78.79	1.89
Isorhamnetin	316.26	2	7	4	120.36	-0.31
Isodihydrosyringetin	348.3	3	8	4	125.68	-0.66

nRB: Number of Rotatable bonds, optimal: 0–10; nHA: Number of Hydrogen bond acceptors, optimal: 0–10; nHD: Number of Hydrogen bond donors, optimal: 0–5; TPSA: Topological Polar Surface Area, optimal: 0-140; LogP: Log of the octanol/water partition coefficient, optimal: ≤5.

Construction of PPI network and core targets of L. sinense

A PPI network consisting of 389 nodes and 4,947 edges was established (Fig. 3A). Based on the threshold values of Degree, BC and CC, with the first screening using Degree ≥ 26, BC ≥ 0.00363 and CC ≥ 0.4228, the PPI network was pruned to 73 nodes and 1,049 edges (Fig. 3B). Subsequently, nodes with Degree ≥ 29, BC ≥ 0.0085 and CC ≥ 0.6324 were screened as the second screening threshold values and resulted in 20 core nodes and 178 edges (Fig. 3C). These 20 targets, namely *AKT1*, *SRC*, *ALB*, *EGFR*, *HSP90AA*, *ESR1*, *VEGFA*, *TNF*, *MTOR*, *HIF1A*, *ERBB2*, *AR*, *SIRT1*, *BCL2L1*, *PPARG*, *GSK3B*, *PTGS2*, *NR3C1*, *PIK3CA* and *HPGDS*, were defined as the core targets of *L. sinense* (Supplementary Table 4), which likely to contribute to its pharmacological activities.

Enrichment analysis of compound targets

The enrichment analysis was performed with GSEApy (*version 1.0.4*) on the 389 compound targets, with a screening threshold of a P value less than 0.05. The results retrieved 202 KEGG pathways (Supplementary Table 5), and 1,875 GO terms. The GO terms were further grouped into Biological Process (1,559 items), Cellular Component (80 items) and Molecular Function (236 items) (Supplementary Table 6). Among the top-ranked enrichment results, several cancer-related pathways were significantly identified in the KEGG pathways, including Pathways in cancer, Chemical carcinogenesis, Prostate cancer, Proteoglycans in cancer and Central carbon metabolism in cancer (Fig. 4A). In addition, HIF-1 signalling pathway and cell cycle were also observed in the KEGG pathways, which consistent with our previous findings that the biological properties of *L. sinense* were associated with G2/M cell cycle arrest and HIF activation [13]. The GO term analysis predicted that the targets of *L. sinense* are mainly related with protein phosphorylation (GO:0006468) in Biological Process, integral component of plasma membrane (GO:0005887) in Cellular Component, and protein tyrosine kinase activity (GO:0004713) in Molecular Function (Fig. 4B). These results suggest a role of *L. sinense* in regulating cancer and cancer-related pathways, indicating its potential as a therapeutic agent in cancer treatment.

CTP network construction and hub connections identification

The top 20 KEGG pathways and their associated targets were selected to construct the TP network (Supplementary Fig. 1). Subsequently, a CTP network was built by incorporating the 15 active compounds, 20 core targets and the top 20 KEGG pathways, and in the end the CTP network consisted of 53 nodes and 195 edges (Fig. 5A). A hub network was identified from the CTP network which containing 20 nodes and 65 edges (Fig. 5B, Supplementary Table 7). Within the hub network, 6 hub targets, namely *AKT1*, *EGFR*, *SRC*, *ESR1* and *GSK3B*, were found to be directly regulated by Apigenin. Additionally, 8 signalling pathways were involved in the hub network. Many of these signalling pathways were related with cancer processes, including Pathways in cancer, Chemical carcinogenesis, Proteoglycans in cancer and Prostate cancer. Furthermore, HIF-1 signalling pathway was also identified in the hub network, indicating a crucial role of HIF-1 signalling pathway in the biological activities of *L. sinense*.

To investigate the associated diseases with the hub targets, an analysis of the DisGeNET database (https://www.disgenet.org/ accessed on 15 May 2023) (*version 7.0*) was performed via the disgenet2r package (*version 0.99.3*) in R. The results revealed that the top enriched diseases were primarily related to breast cancer, such as Breast carcinoma, Mammary neoplasms, Mammary neoplasms and mammary carcinoma (Fig. 5C; Supplementary Table 8). This finding suggests a potential therapeutic role of *L. sinense* in the treatment of breast cancer.

Molecular docking between Apigenin and hub targets

Molecular docking was employed to validate the interactions between Apigenin and 6 hub target proteins. The results presented that Apigenin exhibited a strong molecular docking affinity with 6 hub targets, as evidenced by docking scores of less than − 5 kcal/mol (Table 2). AKT1 displayed the best binding activity with Apigenin (affinity = -9.6), followed by ESR1(affinity = -8.9), PTGS2 (affinity = -8.8), SRC (affinity =

-8.6), EGFR (affinity = -8.5), and GSK3B (affinity = -8.4). The binding structures showed that Apigenin deeply entered the binding sites of each hub target, with abundant hydrogen-bond donors and acceptors around the binding cavity (Fig. 6). The binding sites and interaction bonds of Apigenin with each hub target protein were shown in Table 2. Taking AKT1 as an example, Apigenin bound to site of Ser205 in AKT1 via conventional hydrogen bond, while bound to sites of Asp292, Trp80, Leu210, Leu264, Lys268 and Val270 in AKT1 through pi-anion, pi-pi stacked and pi-alkyl bonds (Fig. 6A).

Table 2
Binding affinities and Receptor-ligand interactions of Apigenin with hub targets

Compound name	Protein	Binding affinity (kcal/mol)	Interaction residues	Interaction bonds
Apigenin	AKT1	-9.6	Ser205, Asp292, Trp80, Leu210, Leu264, Val270, Lys268	Conventional Hydrogen Bond, Pi-Anion, Pi-Pi Stacked, Pi-Alkyl
	EGFR	-8.5	Lys745, Met766, Thr854, Leu777, Val726, Ala743, Cys775, Leu844	Conventional Hydrogen Bond, Unfavorable Donor-Donor, Pi-Lone Pair, Pi-Alkyl
	SRC	-8.6	Asp404, Gly406, Met314, Lys295, Val323, Ala403	Conventional Hydrogen Bond, Carbon Hydrogen Bond, Unfavorable Acceptor-Acceptor, Pi-Anion, Pi-Lone Pair, Pi-Alkyl
	ESR1	-8.9	Glu353, Arg394, His524, Phe404, Leu346, Leu349, Ala350, Leu387, Leu391, Met421, Ile424	Conventional Hydrogen Bond, Carbon Hydrogen Bond, Pi-Pi Stacked, Pi-Alkyl
	GSK3B	-8.4	Cys199, Tyr134, Ile62, Val70, Ala83, Leu188	Pi-Sulfur, Pi-Pi Stacked, Pi-Alkyl
	PTGS2	-8.8	Arg120, Phe518, Val349, Leu352, Ala516, Val523, Ala527	Conventional Hydrogen Bond, Pi-Alkyl

Effects of L. sinense ethanol extract (LSE) on breast cancer cells

In our previous study, we demonstrated that the water extract of *L. sinense* has a significant inhibitory effect on the growth of multiple breast cancer cell lines [13]. Based on the network pharmacology results, we found that Apigenin may play a key role in treating cancer. These represent a new class of compounds, as unlike in our previous study, the Apigenin is almost insoluble in water and is present in the ethanol extract [29], we therefore chose ethanol as the solvent to extract compounds from *L. sinense* in this analysis.

To validate the effect of *L. sinense* ethanol extract (LSE) on breast cancer, an immortalized human breast epithelial cell line MCF10A and 7 breast cancer cell lines (BT20, MDA-MB-157, MDA-MB-231, MDA-MB-468, HCC1395, HCC1806 and HCC1937) were treated with LSE followed by a cell viability assay. The results showed that addition of LSE led to a strong inhibition of growth in multiple of the cell lines tested in a dose-dependent manner at 24 (Fig. 7A) or 48 hours (Fig. 7B) post-treatment. Furthermore, to confirm the effects of LSE on cell viability, a 3D mammosphere assay was performed on MDA-MB-468 cells. The results demonstrated a significant decrease in cell viability ($P < 0.001$) in LSE-treated MDA-MB-468 cells (Fig. 7C). These experiments provide further evidence of the growth inhibitory effect of *L. sinense* on breast cancer.

GEO datasets validation

To gain further insights into the mechanisms of Apigenin against breast cancer, we utilized publicly available GEO datasets on human breast cancer cells with the treatment of Apigenin. 2 GEO datasets were selected based on predetermined screening criteria, which included a total of 14 samples derived from 2 different types of human breast cancer cell lines (Supplementary Table 9).

Differentially expressed genes (DEGs) were screened from the obtained GEO datasets (Supplementary Fig. 2). KEGG enrichment analysis revealed that Breast cancer was significantly enriched from both up- and down-regulated DEGs in MCF7 cells upon Apigenin treatment (Fig. 8A, Supplementary Table 10), highlighting the crucial role of Apigenin in the treatment of breast cancer. Furthermore, the expression levels of genes associated with breast cancer were significantly altered by the treatment of Apigenin (Fig. 8B). In MDA-MB-231 cells, Cell cycle was commonly enriched from both up- and down-regulated DEGs upon Apigenin treatment (Fig. 8D, E, Supplementary Table 11). Notably, genes involved in Pathways in cancer exhibited down-regulated in both MCF7 cells and MDA-MB-231 cells upon Apigenin treatment (Fig. 8C, F), indicating the potential anti-cancer effects of Apigenin. These findings from the GEO dataset analysis further support the role of Apigenin in breast cancer treatment, especially its impact on breast cancer-related pathways, cell cycle regulation, and potential anti-cancer effects through modulation of genes involved in cancer pathways.

Discussion

The anti-tumour activity of *L. sinense* has been previously discussed to be associated with its immunomodulatory activity [6]. In line with these findings, our current analysis highlights the close relationship between the biological activity of *L. sinense* and cancer-related pathways, suggesting a potential role of *L. sinense* in cancer treatment. Moreover, the significant enrichment of the Cell cycle pathway in our analysis further supports our previous findings that the water extract of *L. sinense* leads to cell cycle arrest at the G2/M phase [13]. Additionally, the ethanol extract of *L. sinense* demonstrates a remarkable inhibitory effect on the growth of various breast cancer cell lines, suggesting the considerable potential of *L. sinense* as an adjuvant of therapeutic agent for the treatment of breast cancer.

Most of the active compounds isolated from *L. sinense* showing obvious anti-cancer activity, such as Apigenin [30], Naringenin [31], Luteolin [32], Kaempferol [33] and Quercetin [34], which are flavonoids commonly found in herbal plants and fruits. In our analysis, we identified a hub network consisting of Apigenin interacting with 6 target genes and 8 signalling pathways. Previous studies have reported that the mechanism of anti-cancer property of Apigenin is likely due to its ability to cause cell cycle arrest, trigger apoptosis, induce autophagy, inhibit migration/invasion, attenuate drug resistance, and stimulate immune responses in various cancer types both *in vitro* and *in vivo* [35, 36]. The identified hub network shown that AKT1, EGFR, SRC, ESR1, GSK3B and PTGS2 can directly interact with Apigenin. By using molecular docking method, we observed that Apigenin binding with these hub targets tightly and forming various interaction bonds at the binding sites. We further checked the mRNA expressions of these 6 hub targets in the TCGA cohort using UCSCXenaShiny (v1.1.9) (A comprehensive description of UCSCXenaShiny methodology can be found in reference [37]). The results revealed significant up- or down-regulation of these hub targets in most of the 33 TCGA cancer types in mRNA levels (Supplementary Fig. 3A-F). In addition, these target genes also predicted overall survival in multiple cancer types (Supplementary Fig. 3G). These results suggesting the Apigenin in *L. sinense* may play a key role in regulating cancer process and disease-related signalling pathways.

L. sinense has traditionally been used to replenish blood in the body, and treat conditions such as haemostasis, anaemia, bleeding and menorrhagia in Chinese folk medicine [1]. However, there is no direct evidence to prove the blood-enriching function of *L. sinense* so far. Our previous study demonstrated that the water extract of *L. sinense* exhibits the ability to induce hypoxia inducible factor (HIF) activation [13]. Interestingly, in our current analysis, the HIF-1 signalling pathway was also significantly enriched. Given that HIF-1 signalling plays a key role in angiogenesis and blood vessel proliferation, we propose that the blood-enriching function of *L. sinense* might not by directly increase the number of red blood cells, but through regulating HIF-1 signalling pathway, thereby leading to the expression of erythropoietin (EPO) and promoting the blood vessel development. It is well known that anaemia is a common diagnosis in patients with cancer that may affect both quality of life and survival [38]. Cancer can directly cause or exacerbate anaemia either by suppressing haematopoiesis, cytokine-induced iron sequestration, or reduced red blood cell production [39]. Treatment of anaemia can significantly improve patients' quality of life and potentially enhance clinical outcomes. Therefore, the blood-enriching property of *L. sinense* may help alleviate cancer-related symptoms. Additionally, the immunomodulatory activity of *L. sinense* may play a critical role in this process. However, it is worth noting that the activation of HIF-1 signalling also contributes to tumour cell invasion, suggesting a bidirectional regulatory role of the HIF-1 signalling pathway in both blood enrichment and tumour progression. Further exploration and verification are required to elucidate the mechanisms underlying these effects and to better understand the blood-enriching and anti-tumour activities of *L. sinense*.

Conclusions

Our study predicts that the biological activities of *L. sinense* are strongly associated with breast cancer and multiple cancer-related pathways. The active compound Apigenin in *L. sinense* appears to have a

crucial role against cancer. Experimental evaluations of the ethanol extract of *L. sinense* have demonstrated a significant inhibitory effect on multiple breast cancer cell lines. GEO datasets validation indicates the involvement of breast cancer upon treatment with Apigenin in human breast cancer cells. These findings highlight the potential of *L. sinense* as a promising therapeutic agent for the treatment of breast cancer. Further research and clinical investigations are warranted to explore the full therapeutic potential of *L. sinense* in combating breast cancer.

Abbreviations

2D, Two dimensional; 3D, Three dimensional; GEO, Gene Expression Omnibus; GO, Gene Ontology; KEGG, Kyoto Encyclopedia of Genes and Genomes; *L. sinense, Limonium Sinense* (Girard) Kuntze; LSE, *L. sinense* ethanol extract.

Declarations

Acknowledgment

We thank all authors for their contributions and support.

Authors' contributions

YW and JW designed the study. HZ and SW performed the experiments. YW, JW, HZ and SW analysed the data and finalised the figures, and all other authors contributed to data interpretation. YW, JW, HZ, PTFW, RME and XT drafted the manuscript with input from other authors. All authors read and approved the final manuscript.

Funding

This project was funded in part by Yancheng Teachers' University and the University of Southampton. YW was supported by the Medical Research Council [grant no: MR/S025480/1] and an Academy of Medical Sciences/the Wellcome Trust Springboard Award [grant no: SBF002\1038]. SW was supported by China Scholarship Council. For the purpose of open access, the authors have applied a CC-BY public copyright license to any Author Accepted Manuscript version arising from this submission.

Availability of data and materials

All data generated or analysed in this study are included in the article and its supplementary information files.

Ethics approval and consent to participate

Not applicable.

Consent for publication

All authors agree to publish this paper.

Competing interests

The authors declare that they have no relevant conflict of interest or personal relationships that could have appeared to influence the work reported in this paper.

References

1. Dong, B., *Research on the conservation of Limonium sinense in the coast of Jiangsu.* Chin Wild Plant Res, 2005. **24**(06): p. 28-30.
2. Chaung, S.S., et al., *The hepatoprotective effects of Limonium sinense against carbon tetrachloride and beta-D-galactosamine intoxication in rats.* Phytother Res, 2003. **17**(7): p. 784-91.
3. Wu, Z.Y.P.H.R., *Flora of China*, ed. Z.Y.P.H.R. Wu. Vol. 15. 1996: Science Press (Beijing) & Missouri Botanical Garden Press (St. Louis).
4. Li, H., *Plumbaginaceae.* Flora of Taiwan, 1998. **4**: p. 79-82.
5. College, J.N.M., *Chinese Materia Medica Dictionary*. 1977, Shanghai Press of Science and Technology Shanghai.
6. Tang, X.H., et al., *Antitumor and immunomodulatory activity of polysaccharides from the root of Limonium sinense Kuntze.* Int J Biol Macromol, 2012. **51**(5): p. 1134-9.
7. Tang, X.H., et al., *Isolation and identification of anti-tumor polysaccharide LSP21 from Limonium sinense (Girard) Kuntze.* Int J Biol Macromol, 2014. **70**: p. 138-42.
8. Tang, X.H., et al., *Mitochondrial modulation is involved in the hepatoprotection of Limonium sinense extract against liver damage in mice.* J Ethnopharmacol, 2008. **120**(3): p. 427-31.
9. Tang, X.H., et al., *Preservation on calcium homeostasis is involved in mitochondrial protection of Limonium sinense against liver damage in mice.* Pharmacogn Mag, 2010. **6**(23): p. 191-7.
10. Hsu, W.C., et al., *Limonium sinense and gallic acid suppress hepatitis C virus infection by blocking early viral entry.* Antiviral Res, 2015. **118**: p. 139-47.
11. Kuo, Y.C., et al., *Samarangenin B from Limonium sinense suppresses herpes simplex virus type 1 replication in Vero cells by regulation of viral macromolecular synthesis.* Antimicrob Agents Chemother, 2002. **46**(9): p. 2854-64.
12. Lin, L.C., Y.C. Kuo, and C.J. Chou, *Anti-herpes simplex virus type-1 flavonoids and a new flavanone from the root of Limonium sinense.* Planta Med, 2000. **66**(4): p. 333-6.
13. Zhao, H., et al., *Integrated analysis reveals effects of bioactive ingredients from Limonium Sinense (Girard) Kuntze on hypoxia-inducible factor (HIF) activation.* Front Plant Sci, 2022. **13**: p. 994036.
14. Lin, L.C. and C.J. Chou, *Flavonoids and phenolics from Limonium sinense.* Planta Med, 2000. **66**(4): p. 382-3.

15. Ru, J., et al., *TCMSP: a database of systems pharmacology for drug discovery from herbal medicines.* J Cheminform, 2014. **6**: p. 13.
16. Xu, H.Y., et al., *ETCM: an encyclopaedia of traditional Chinese medicine.* Nucleic Acids Res, 2019. **47**(D1): p. D976-D982.
17. Ghose, A.K., V.N. Viswanadhan, and J.J. Wendoloski, *A knowledge-based approach in designing combinatorial or medicinal chemistry libraries for drug discovery. 1. A qualitative and quantitative characterization of known drug databases.* J Comb Chem, 1999. **1**(1): p. 55-68.
18. Veber, D.F., et al., *Molecular properties that influence the oral bioavailability of drug candidates.* J Med Chem, 2002. **45**(12): p. 2615-23.
19. Missiuro, P.V., et al., *Information flow analysis of interactome networks.* PLoS Comput Biol, 2009. **5**(4): p. e1000350.
20. Raman, K., N. Damaraju, and G.K. Joshi, *The organisational structure of protein networks: revisiting the centrality-lethality hypothesis.* Syst Synth Biol, 2014. **8**(1): p. 73-81.
21. Huang da, W., B.T. Sherman, and R.A. Lempicki, *Systematic and integrative analysis of large gene lists using DAVID bioinformatics resources.* Nat Protoc, 2009. **4**(1): p. 44-57.
22. Wan, Y., et al., *Utilising network pharmacology to explore the underlying mechanism of Wumei Pill in treating pancreatic neoplasms.* BMC Complement Altern Med, 2019. **19**(1): p. 158.
23. Fang, Z., X. Liu, and G. Peltz, *GSEApy: a comprehensive package for performing gene set enrichment analysis in Python.* Bioinformatics, 2023. **39**(1).
24. Pinero, J., et al., *The DisGeNET knowledge platform for disease genomics: 2019 update.* Nucleic Acids Res, 2020. **48**(D1): p. D845-D855.
25. Chin, C.H., et al., *cytoHubba: identifying hub objects and sub-networks from complex interactome.* BMC Syst Biol, 2014. **8 Suppl 4**(Suppl 4): p. S11.
26. Ertay, A., et al., *WDHD1 is essential for the survival of PTEN-inactive triple-negative breast cancer.* Cell Death Dis, 2020. **11**(11): p. 1001.
27. Liu, H., et al., *SGLT1 is required for the survival of triple-negative breast cancer cells via potentiation of EGFR activity.* Mol Oncol, 2019. **13**(9): p. 1874-1886.
28. Wang, Y., et al., *ASPP2 controls epithelial plasticity and inhibits metastasis through beta-catenin-dependent regulation of ZEB1.* Nat Cell Biol, 2014. **16**(11): p. 1092-104.
29. Eroglu Ozkan, E., et al., *The Therapeutic Potential of Ethnomedicinally Important Anatolian Thyme Species: A Phytochemical and Biological Assessment.* Front Pharmacol, 2022. **13**: p. 923063.
30. Zhou, Y., et al., *Apigenin in cancer therapy: From mechanism of action to nano-therapeutic agent.* Food Chem Toxicol, 2022. **168**: p. 113385.
31. Motallebi, M., et al., *Naringenin: A potential flavonoid phytochemical for cancer therapy.* Life Sci, 2022. **305**: p. 120752.
32. Lin, Y., et al., *Luteolin, a flavonoid with potential for cancer prevention and therapy.* Curr Cancer Drug Targets, 2008. **8**(7): p. 634-46.

33. Wang, X., et al., *The mechanism of anticancer action and potential clinical use of kaempferol in the treatment of breast cancer.* Biomed Pharmacother, 2019. **117**: p. 109086.
34. Tang, S.M., et al., *Pharmacological basis and new insights of quercetin action in respect to its anti-cancer effects.* Biomed Pharmacother, 2020. **121**: p. 109604.
35. Madunic, J., et al., *Apigenin: A dietary flavonoid with diverse anticancer properties.* Cancer Lett, 2018. **413**: p. 11-22.
36. Yan, X., et al., *Apigenin in cancer therapy: anti-cancer effects and mechanisms of action.* Cell Biosci, 2017. **7**: p. 50.
37. Wang, S., et al., *UCSCXenaShiny: an R/CRAN package for interactive analysis of UCSC Xena data.* Bioinformatics, 2022. **38**(2): p. 527-529.
38. Anand, S., A. Burkenroad, and J. Glaspy, *Workup of anemia in cancer.* Clin Adv Hematol Oncol, 2020. **18**(10): p. 640-646.
39. Dicato, M., L. Plawny, and M. Diederich, *Anemia in cancer.* Ann Oncol, 2010. **21 Suppl 7**: p. vii167-72.

Figures

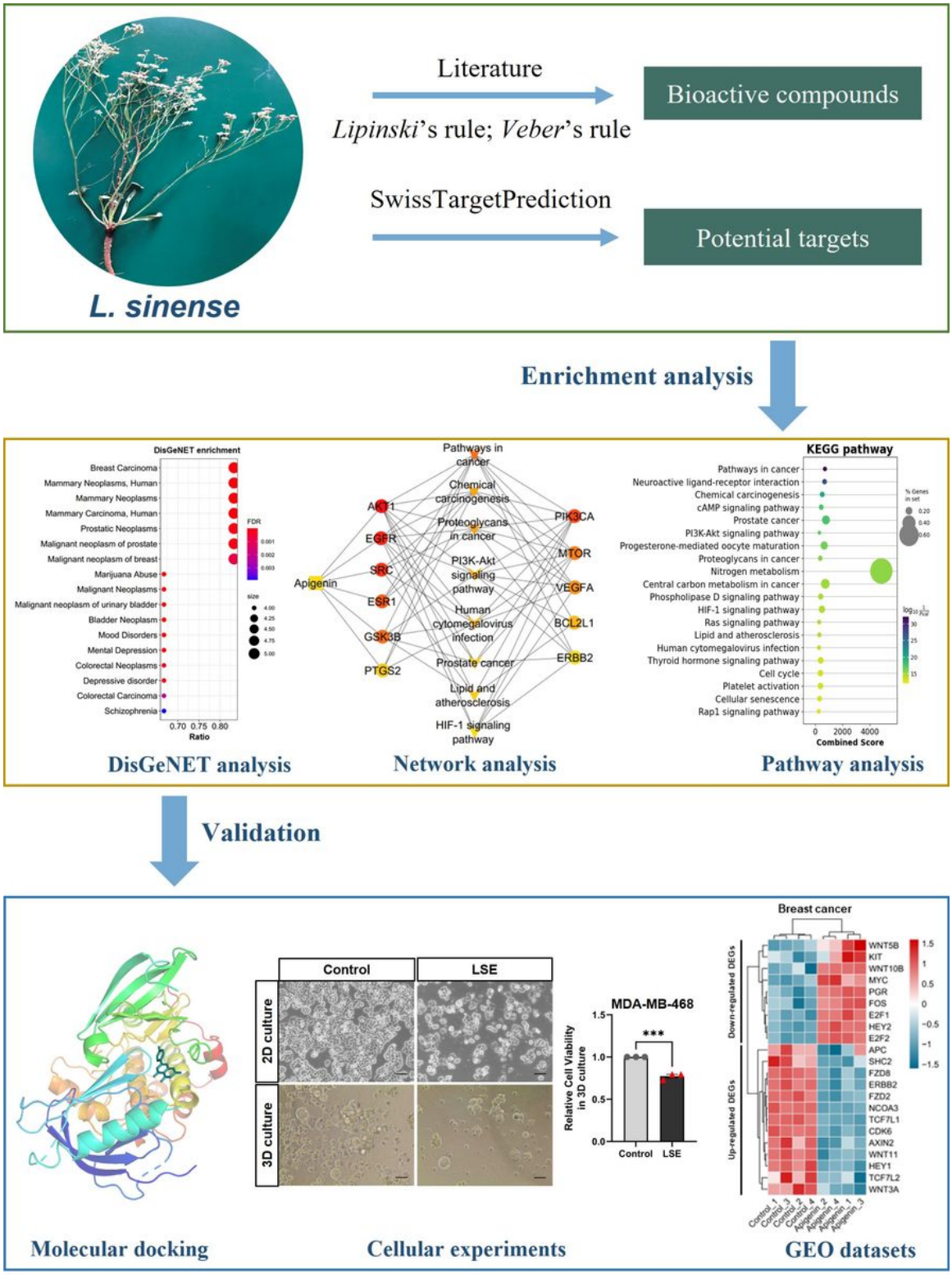

Figure 1

Flow chart of the study.

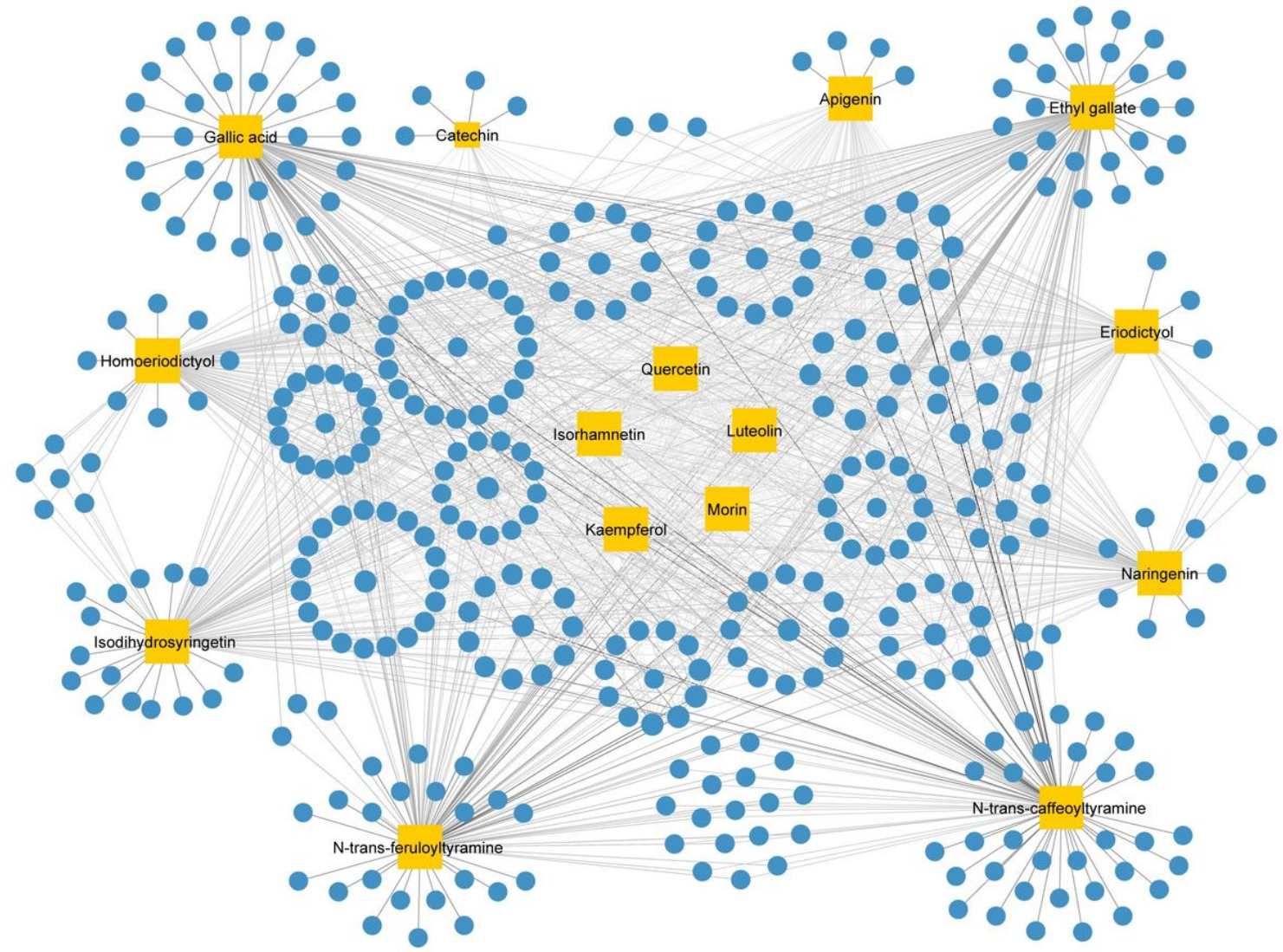

Figure 2

Compound-Target (CT) network of *L. sinense*. Graph consists of 15 compounds and 389 compound-related targets. The orange rectangles represent the small molecular components in *L. sinense*. The blue circles represent the relevant targets. The edges represent the relationship between compounds and target nodes. The node size is proportional to the node degree in the network, and the width and colour of the edges is proportional to the edge betweenness centrality.

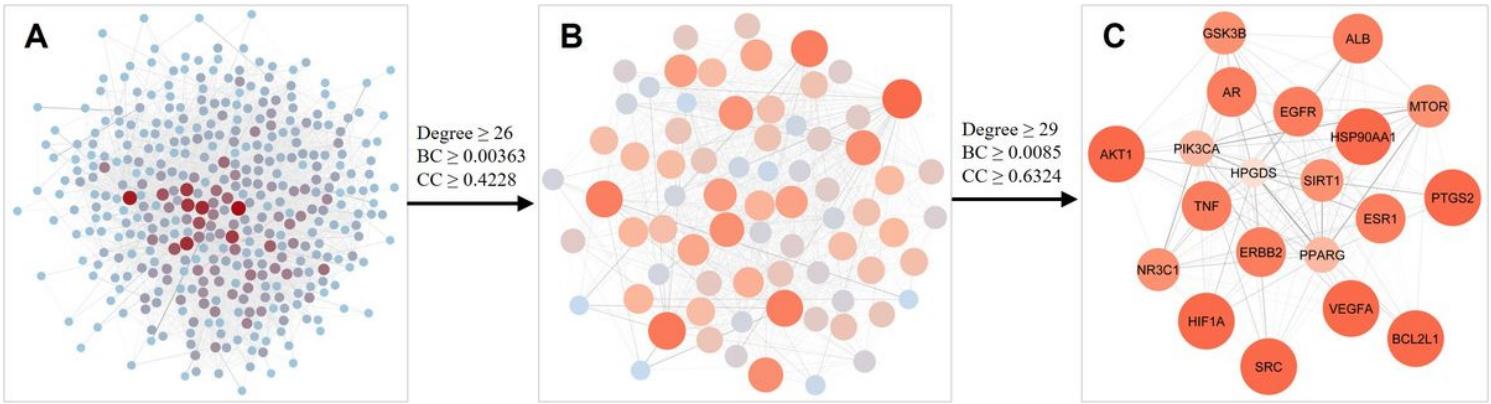

Figure 3

The process of topological screening for the PPI network. Each node represents a protein and each edge refers an interaction. The size and colour of the nodes represent the node degree in the network, and the width and colour of the edges represent the edge betweenness centrality. The core targets were screened based on the Degree, betweenness centrality (BC) and closeness centrality (CC) values in the network.

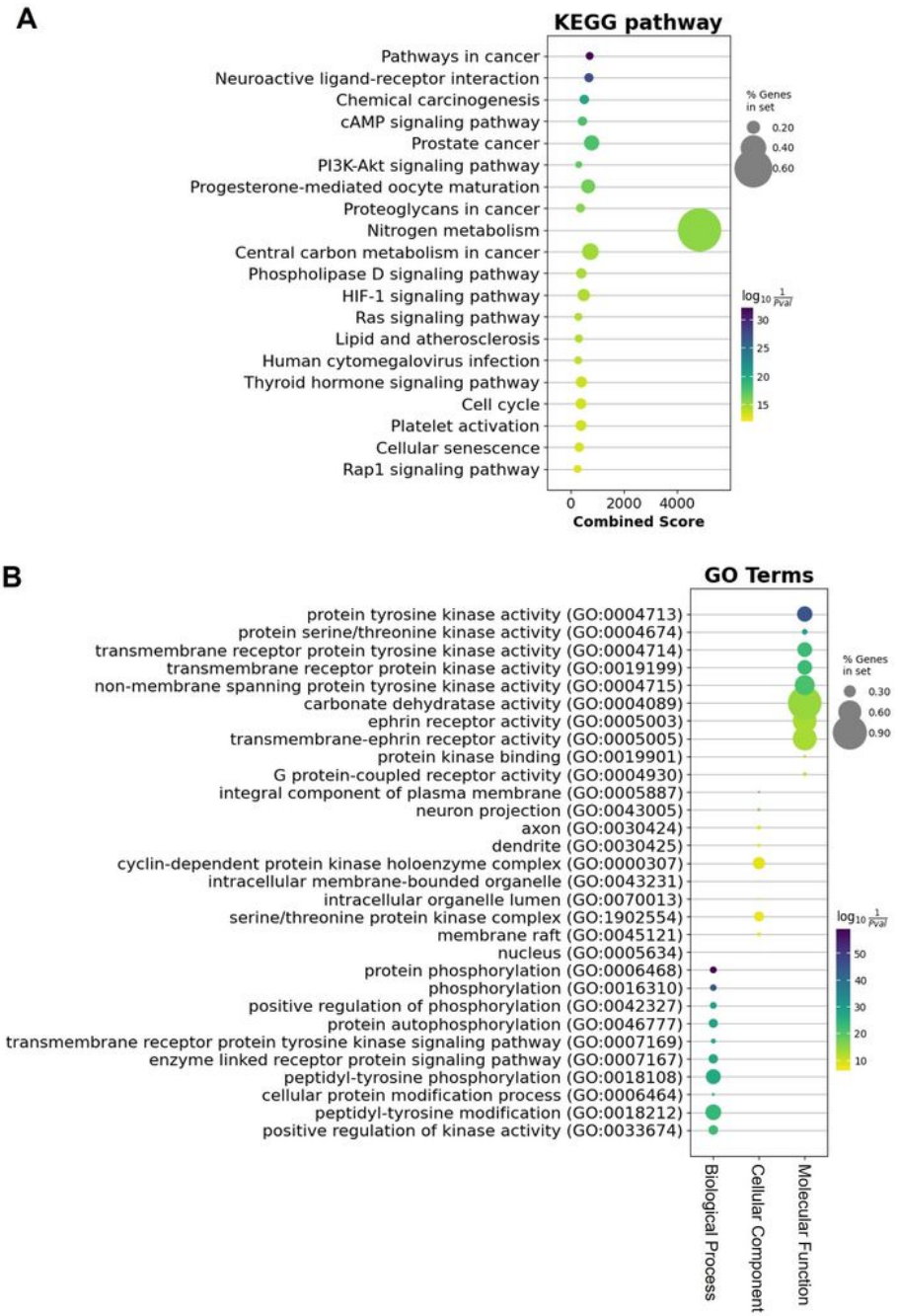

Fig. 4 Enrichment analysis from *L. sinense* targets. (**A** and **B**) Scatter plots showing the Kyoko Encyclopedia of Genes and Genomes (KEGG) pathways (Top20) and Gene Ontology (GO) terms (Top10 of each category) enriched by the *L. sinense* potential targets. The GO term was further categorised into Biological Process, Cellular Component and Molecular Function. The sizes of circles represent the percentage of genes in the gene set, and the colours of circles represent the $\log_{10}(\frac{1}{Pvalue})$. Combined score is defined by the Enrichr.

Figure 4

See image above for figure legend.

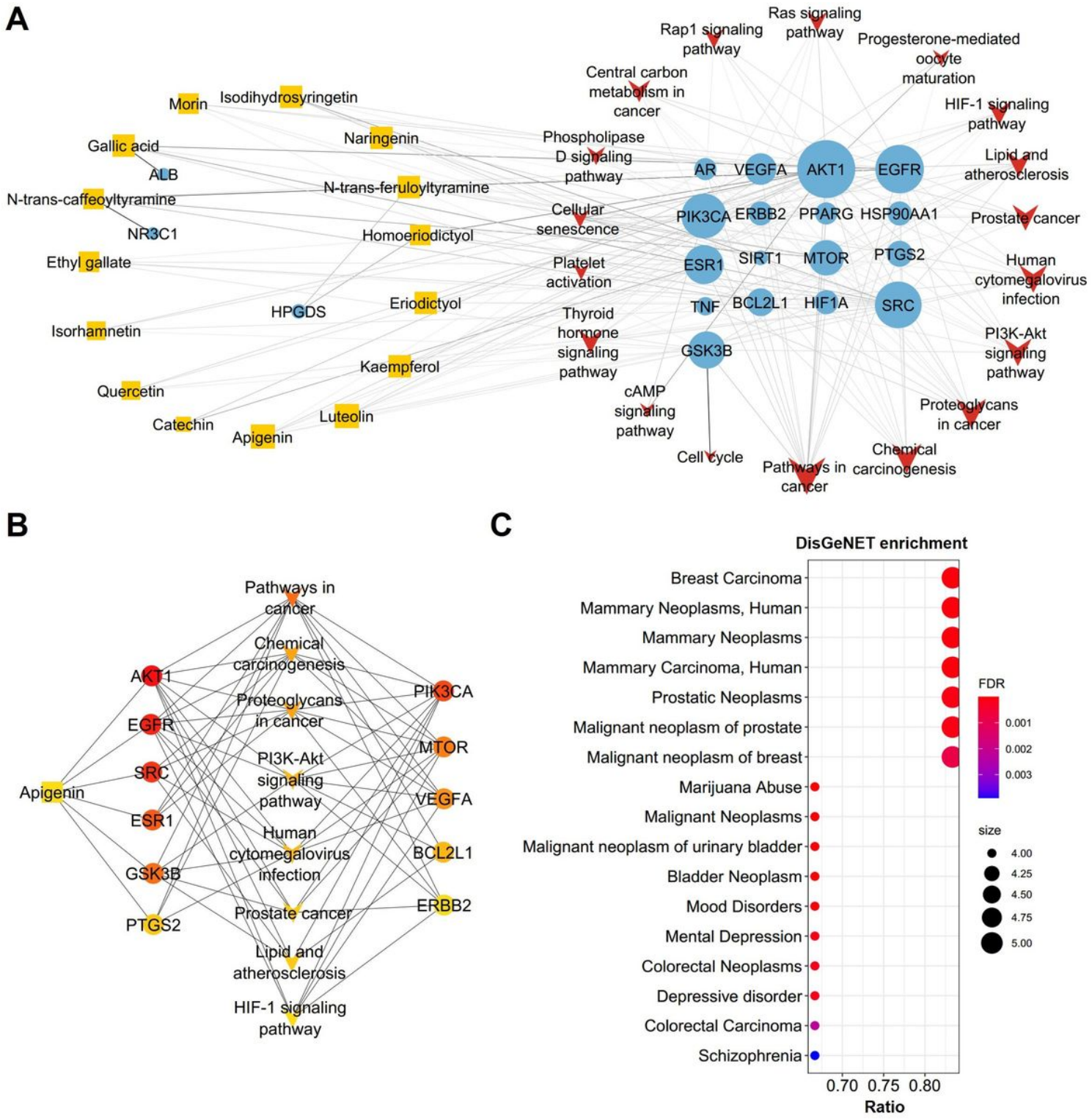

Figure 5

Hub network and DisGeNET enrichment analysis. (**A**) Compound-Target-Pathway network of *L. sinense*. The orange rectangles represent the small molecular components in *L. sinense*. The blue circles represent

the relevant targets. The red V nodes represent the relevant signalling pathways.The edges represent the relationship among compounds, targets and pathways. The node size is proportional to the node degree in the network, and the width and colour of the edges is proportional to the edge betweenness centrality. (**B**) Hub network identified from the CTP network using the CytoHubba. Colour node indicates the degree value of each node in the network. (**C**) DisGeNET enrichment analysis of hub targets. The size of the dots refers to the number of genes enriched for that disease (the greater the number of genes, the larger the dot). The FDR is defined by a colour scale, the closer it is to red, the greater the FDR value and the greater the association.

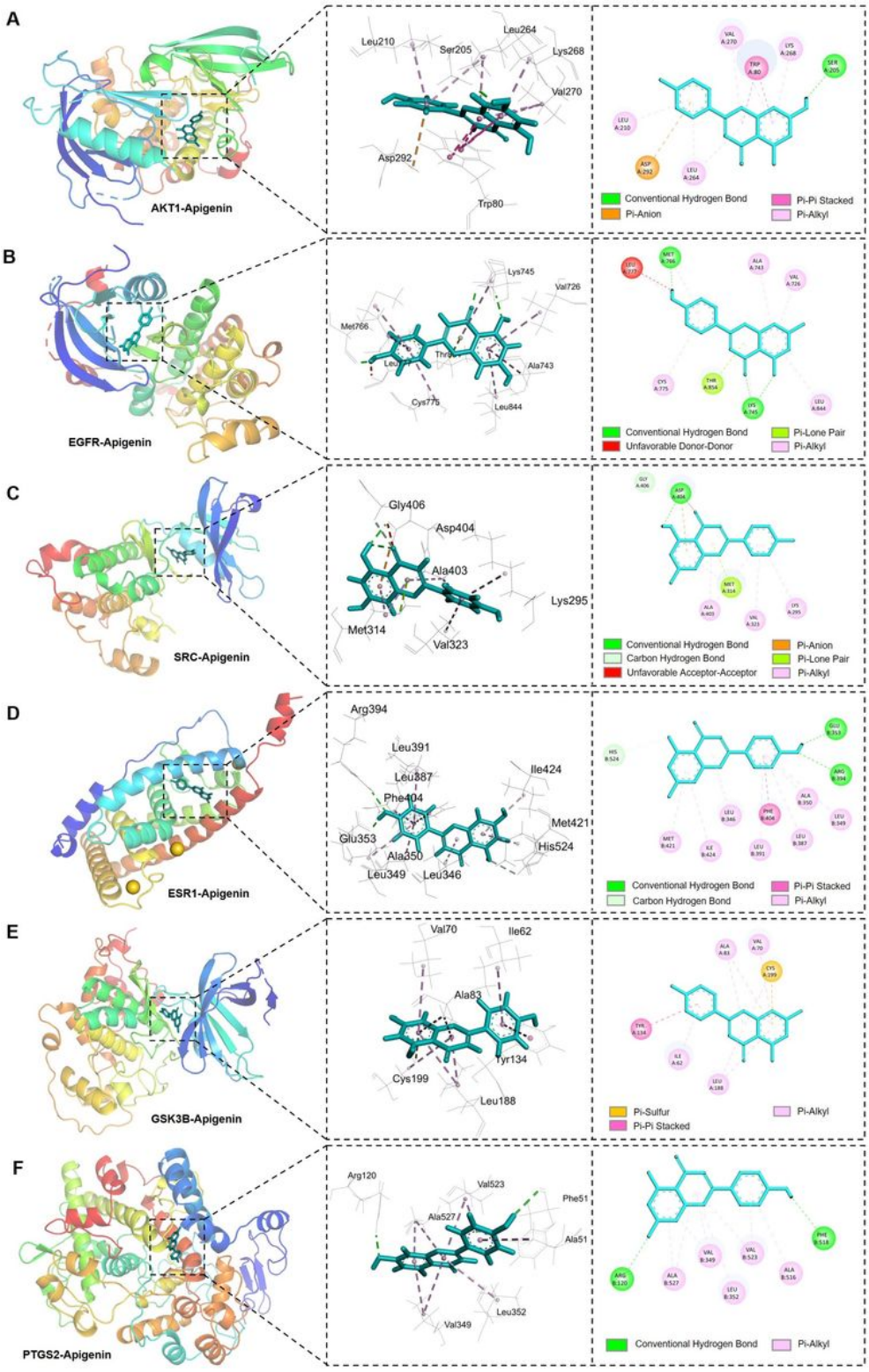

Figure 6

Molecular docking analysis of Apigenin with hub target proteins. (**A-F**) Graphs showing the binding mode and molecular interactions of Apigenin with AKT1, EGFR, SRC, ESR1, GSK3B and PTGS2, respectively. The 3D graphs showing the binding model of Apigenin and each target. The 2D graphs showing the specific interactions between Apigenin and the hub targets.

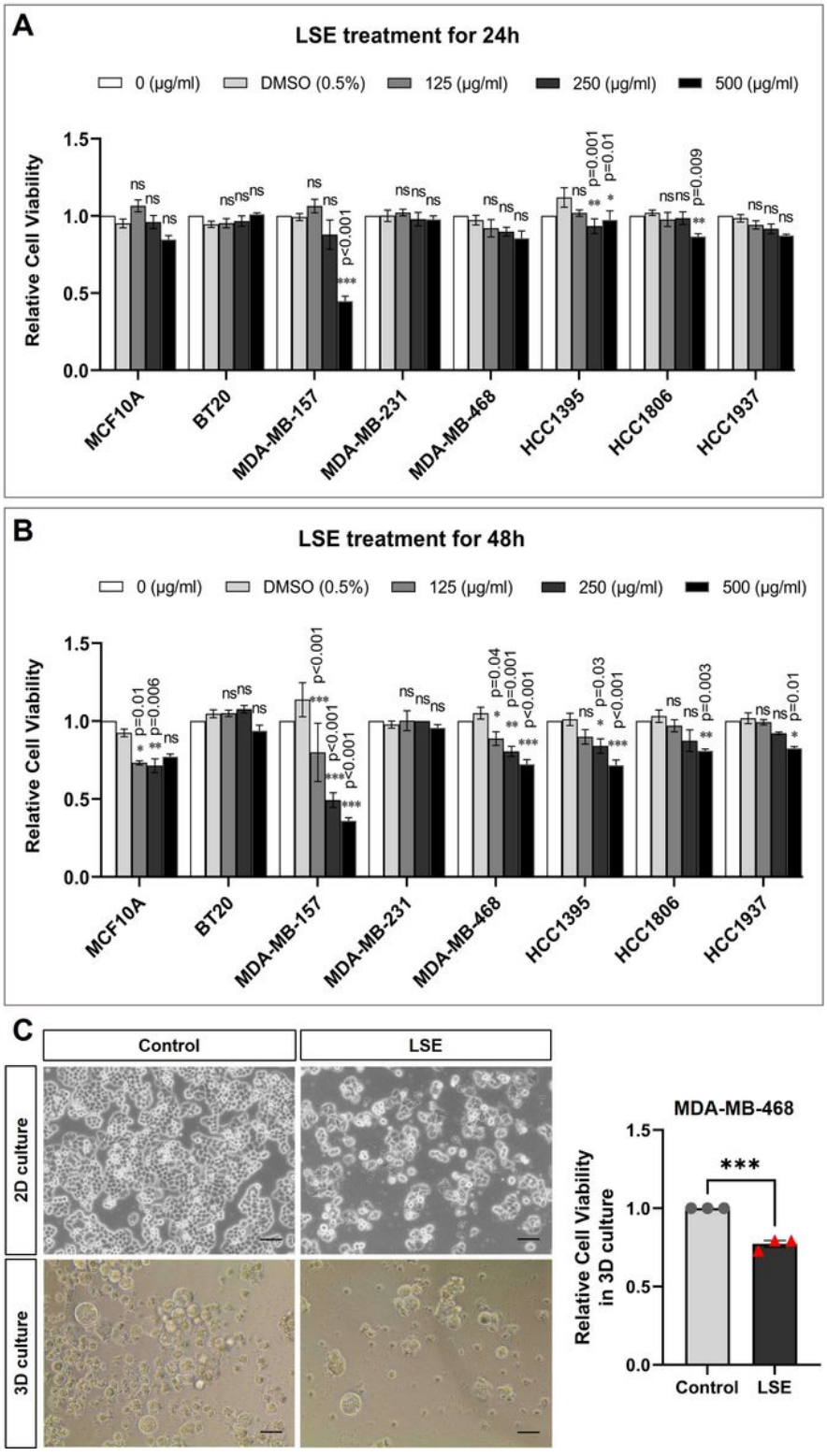

Figure 7

Cell viability assay of ethanol extract of *L. sinense* (LSE) on breast cancer cells. (**A** and **B**) Graphs showing relative cell viability in multiple cell lines treated with *L. sinense* ethanol extract (LSE) at the indicated concentration for 24 (**A**) or 48 hours (**B**). Cell-Titer Glo® assay was performed to measure cell viability. Data are mean ± SEM; n = 3 samples per group. ns, not significant; *P < 0.05; **P < 0.01 and ***P < 0.001 by the Two-way ANOVA. (**C**) Representative phase contrast microscopy images showing the

morphology change of MDA-MB-468 cells treatment with LSE in 2D and 3D cultures. Scale bar: 50 μm. Bar plot showing the relative cell viability change (Cell-Titer Glo® assay) of MDA-MB-468 cells with indicated treatment in 3D culture. Data are mean ± SEM. ns, not significant; *P < 0.05; **P< 0.01 by the Student's t-test.

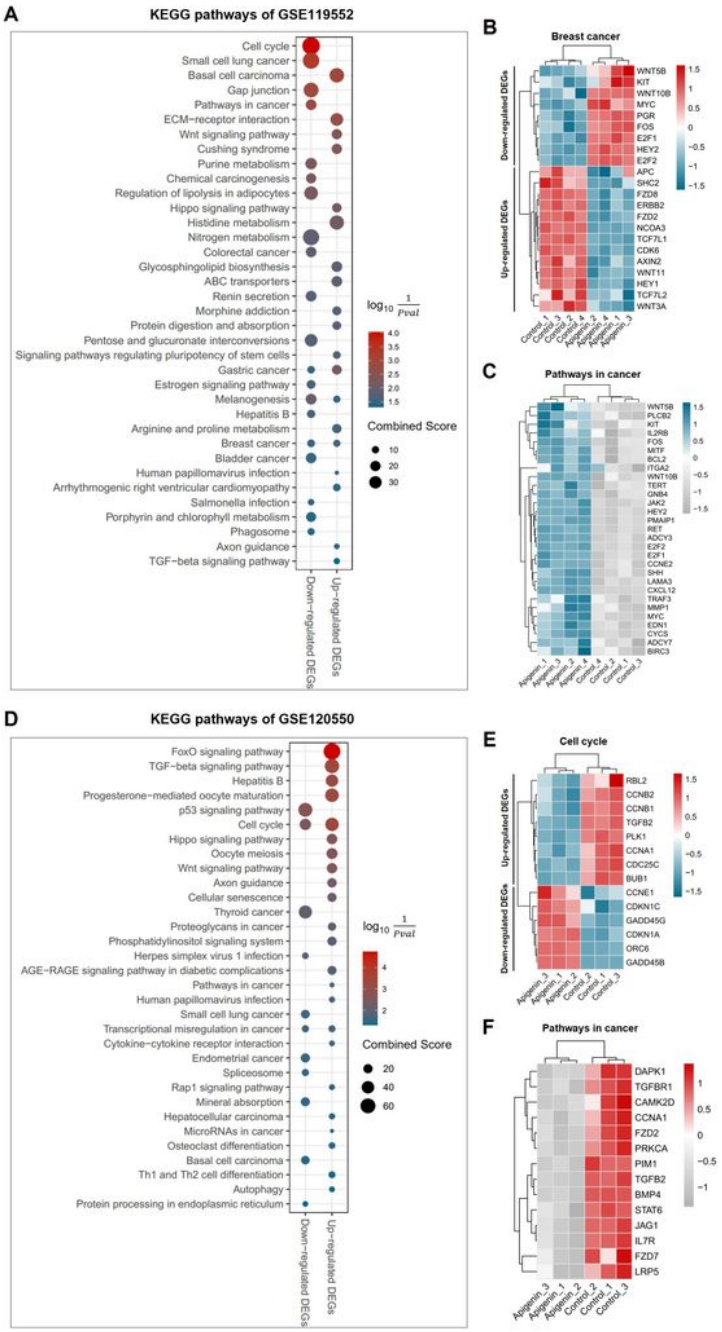

Fig. 8 Validation of Apigenin treatment on human breast cancer cells using GEO datasets. (A, D) Scatter plots illustrating the significant KEGG pathways enriched by the up- and down-regulated differentially expressed genes (DEGs) within indicated GEO datasets. The y-axis represents the name of pathway, and the x-axis represents the up- and down-regulated DEGs. Dot size represents the combined score, and the colour indicates the $\log10(\frac{1}{Pvalue})$. **(B, C, E, F)** Heatmaps showing transcriptional levels of genes enriched in each representative pathway of Apigenin-treated breast cancer cells compared to vehicle.

Figure 8

See image above for figure legend.

Supplementary Files

This is a list of supplementary files associated with this preprint. Click to download.

- SupplementaryTable1.docx
- SupplementaryTable10.xlsx
- SupplementaryTable11.xlsx
- SupplementaryTable12.txt
- SupplementaryTable2.xlsx
- SupplementaryTable3.xlsx
- SupplementaryTable4.xlsx
- SupplementaryTable5.xlsx
- SupplementaryTable6.xlsx
- SupplementaryTable7.xlsx
- SupplementaryTable8.txt
- SupplementaryTable9.docx
- SupplementaryMaterials.docx